

# Iron abundance in hot hydrogen-deficient central stars and white dwarfs from FUSE, HST, and IUE spectroscopy<sup>\*</sup>

S. Miksa<sup>1,2</sup>, J.L. Deetjen<sup>1</sup>, S. Dreizler<sup>1</sup>, J.W. Kruk<sup>3</sup>, T. Rauch<sup>1</sup>, and K. Werner<sup>1</sup>

<sup>1</sup> Institut für Astronomie und Astrophysik, Universität Tübingen, Germany  
e-mail: [werner@astro.uni-tuebingen.de](mailto:werner@astro.uni-tuebingen.de)

<sup>2</sup> Institut für Physik der Atmosphäre, DLR Oberpfaffenhofen, Germany  
e-mail: [Sabine.Miksa@dlr.de](mailto:Sabine.Miksa@dlr.de)

<sup>3</sup> Department of Physics and Astronomy, Johns Hopkins University, Baltimore, MD 21218, U.S.A.  
e-mail: [kruk@pha.jhu.edu](mailto:kruk@pha.jhu.edu)

Received date; accepted date

**Abstract.** We present a first systematic investigation of the iron abundance in very hot ( $T_{\text{eff}} \geq 50\,000$  K) hydrogen-deficient post-AGB stars. Our sample comprises 16 PG1159 stars and four DO white dwarfs. We use recent FUSE observations as well as HST and IUE archival data to perform spectral analyses with line blanketed NLTE model atmospheres. Iron is not detected in any PG1159 star. In most cases this is compatible with a solar iron abundance due to limited quality of HST and IUE data, although the tendency to an iron underabundance may be recognized. However, the absence of iron lines in excellent FUSE spectra suggests an underabundance by at least 1 dex in two objects (K 1-16, NGC 7094). A similar result has been reported recently in the [WC]-PG1159 transition object Abell 78 (Werner et al. 2002). We discuss dust fractionation and s-process neutron-captures as possible origins. We also announce the first identification of sulfur in PG1159 stars.

**Key words.** Stars: AGB and post-AGB – Stars: atmospheres – Stars: abundances – Stars: evolution – White dwarfs – Ultraviolet: stars

## 1. Introduction

PG1159 stars are hot ( $T_{\text{eff}}=65\,000\text{--}180\,000$  K) hydrogen-deficient post-AGB stars with carbon, helium and oxygen as main atmospheric constituents. They are thought to be the result of a late helium shell flash (see e.g. Werner 2001). Since they belong to the disk population and since diffusion effects can be excluded due to ongoing mass-loss, one expects solar iron abundances.

Up to now no iron abundances were determined for these objects, for two reasons. First, iron is highly ionized so that spectral lines have to be looked for in the UV and FUV region. High resolution, high-S/N spectra are required from these mostly faint objects. A few of the brightest were observed with IUE, however, line identification is doubtful or impossible, as we will show. HST spectra of many PG1159 stars are archived; however, in most cases the spectral resolution is not high. In this paper we use all this archival material to make a systematic investigation of iron lines with NLTE model atmospheres. We also use new

FUSE spectra of seven PG1159 stars and of the hottest known DO white dwarf for this purpose. Second, spectral analyses require NLTE model atmospheres. Models that include iron opacities for high ionization stages have only recently become available.

## 2. Sample selection and observational data

Our sample comprises all PG1159 stars for which HST and IUE high resolution archival spectra with a minimum acceptable S/N are available. These are 16 out of the 35 objects known. FUSE spectra are available for seven of the program stars. The sample is augmented by four hot non-DA (DO) white dwarfs in order to complete an earlier analysis of DO spectra (Dreizler 1999). The twenty program stars are listed in Table 1. The spectra used for our analysis are listed in Table 2.

### 2.1. FUSE

The FUSE datasets in programs P132 and Q109 were observed for the present study of PG1159 stars, the datasets in program P104 were observed for ISM studies, and the datasets in program M107 were observed for the FUSE cal-

*Send offprint requests to:* K. Werner

<sup>\*</sup> Based on observations obtained with the Far Ultraviolet Spectroscopic Explorer (FUSE), the Hubble Space Telescope (HST), and the International Ultraviolet Explorer (IUE)

**Table 1.** Atmospheric parameters of the program stars as taken from the literature. The iron abundance is determined in this work, except for Abell 78. Abundances are given in % number fractions, except for iron. The iron abundance in PG1159 stars is the logarithm of mass fraction relative to the solar value. For the DO stars Fe is given as number ratio relative to He. Pulsating PG1159 stars are marked with an asterisk

Object	type	$T_{\text{eff}}$ [kK]	$\log g$ (cgs)	H	He	C	N	O	$\log \text{Fe}/\text{Fe}_{\odot}$ (mass fraction)	ref.
RX J 2117.1+3412	PG1159*	170	6.0		61	31		8	$\leq 0$	A
PG1520+525	PG1159	150	7.5		72	21	$< 0.01$	7	$< -0.5$	L
NGC 246	PG1159*	150	5.7		85	13		2	$\leq 0$	H
PG1159-035	PG1159*	140	7.0	$< 5$	61	30	1	8	$< -0.5$	K,L
K 1-16	PG1159*	140	6.4		61	31		8	$< -1.0$	I
HS2324+397	PG1159*	130	6.2	61	30	9	$< 0.1$	0.2	$< -0.5$	D
Abell 43	PG1159*	110	5.7	74	22	4			$\leq 0$	G
Abell 78	PG1159	110	5.5		62	31		7	$< -1.5$	J,M
NGC 7094	PG1159*	110	5.7	74	22	4			$< -1.5$	G
PG1424+535	PG1159	110	7.0		76	22	$< 0.001$	2	$\leq 0$	L
HS1517+7403	PG1159	110	7.0		95	5	$< 0.001$	0.5	$\leq 0$	L
PG2131+066	PG1159*	95	7.5		71	21	1	7	$\leq 0$	L
MCT0130-1937	PG1159	90	7.5		90	9	$< 0.001$	1	$\leq 0$	L
PG1707+427	PG1159*	85	7.5		71	21	1	7	$\leq 0$	L
PG0122+200	PG1159*	80	7.5		71	21	1	7	$\leq 0$	L
HS0704+6153	PG1159	75	7.0		88	9	$< 0.001$	3	$\leq 0$	L
									Fe/He (number ratio)	
KPD 0005+5106	DO	120	7.0		100	0.1	0.01	$< 10^{-5}$	$< 10^{-5}$	A
PG1034+001	DO	100	7.5	$< 5$	100	0.001	0.063	0.0079	$1 \cdot 10^{-5}$	B,C
HZ21	DO	53	7.8	$< 10$	100	$< 0.001$	$< 0.001$	$< 0.001$	$< 10^{-4}$	E
HD149499B	DO	50	8.0	18	82	0.001			$< 10^{-5}$	E,F

References in last column: A: Werner et al. 1996, B: Werner 1996, C: Werner et al. 1995, D: Dreizler et al. 1996, E: Dreizler & Werner 1996, F: Napiwotzki et al. 1995, G: Dreizler et al. 1997, H: Rauch & Werner 1997, I: Kruk & Werner 1998, J: Werner & Koesterke 1992, K: Werner et al. 1991, L: Dreizler & Heber 1998, M: Werner et al. 2002

ibration program. Each of these datasets is available from the Multimission Archive at the Space Telescope Science Institute (MAST). All observations were obtained using the  $30'' \times 30''$  LWRs spectrograph aperture. The data were obtained in “timetag” mode, except for P1320501 and M1070201,2,3 datasets, which were obtained in “histogram” (or spectral image) mode. These datasets were all reduced using the standard CALFUSE pipeline, version 1.8.7. These observations exhibit RMS variations in observed flux that are usually less than 1% from one exposure to another, indicating that no significant signal was lost as a result of channel misalignments. The one exception was SiC1 data for exposure 1 of the observation of RX J 2117.1+3412, for which the flux level was about 20% below that of the other exposures. A description of the FUSE instrument and the channel alignment issues are given by Moos et al. (2000) and Sahnou et al. (2000). For most objects the spectra obtained in different exposures were coaligned by cross-correlating on regions containing narrow interstellar absorption features before combining to produce a spectrum for an entire observation. The resulting spectral resolution was typically about  $20 \text{ km s}^{-1}$ . The spectra obtained in single exposures for the objects HS2324+397 and PG1707+427 did not have

sufficient signal-to-noise ratios to permit cross-correlation, so these spectra were combined without coalignment. In these cases the spectral resolution was somewhat worse, about  $25 \text{ km s}^{-1}$  for PG1707+427, and  $25\text{--}30 \text{ km s}^{-1}$  for HS2324+397.

The observation of K 1-16 required special processing. This observation was obtained during in-orbit checkout very early in the mission, as part of a test to determine both the channel alignment offsets and the primary mirror to spectrograph slit focus offset for each channel. The test consisted of slewing the telescope in  $40 \text{ } 1''$  steps during each exposure, centered on the LiF1 LWRs aperture. There were a total of 11 scans each in the dispersion and cross-dispersion directions. Because the channels were only crudely aligned at the time of this test, the effective exposure time varied for each channel, from about 38 ksec for LiF1 to only 8 ksec for SiC2. Data were discarded for time periods in which the star was outside of the aperture, or for which the count rate otherwise deviated significantly from the mean. These data were processed using version 1.7.7 of CALFUSE, but the differences between this version and 1.8.7 were not significant for the purposes of this program. Custom processing was added to the pipeline to correct the recorded photon positions for the slewing of the

**Table 2.** List of spectra for the program stars. The IUE spectra cover a wavelength range of 1150-1980 Å with a resolution of about 0.1 Å. The available FUSE spectra cover 905-1187 Å with a resolution of about 0.05 Å

Object	— HST —				— IUE —		— FUSE —	
	dataset name	$\lambda$ -range [Å]	res. [Å]	$t_{\text{exp}}$ [min]	SWP number	$t_{\text{exp}}$ [min]	dataset name	$t_{\text{exp}}$ [min]
RX J 2117.1+3412	Z27J0206T	1227–1263	0.06	13	47556	360	P1320501	137
	Z27J0207N	1273–1309	0.06	11	47563	362		
	Z27J0208T	1343–1379	0.06	16	55411	363		
PG1520+525 NGC 246	Z2T20104T	1165–1461	0.60	24			P1320101	81
					03353	112		
					41997	120		
					42068	223		
					42073	115		
					42104	150		
					42214	150		
					42247	120		
					47843	165		
					47844	155		
PG1159-035					23032	1020	Q1090101	105
					53903	667		
					54675	875		
					54976	880		
K 1-16	Z1EJ0304M	1497–1532	0.06	13			I8110302	665
	Z1EJ0305M	1525–1560	0.06	13				
HS2324+397 Abell 43 Abell 78	Z3GW0204T	1140–1436	0.60	74			P1320601	67
	Z3GW0304T	1139–1435	0.60	71	38955	385		
					16967	40		
					19879	425		
NGC 7094					19906	420	P1043701	386
	Z3GW0104T	1139–1435	0.60	22	52919	330		
	Z3GW0105T	1455–1751	0.60	47	56107	400		
					56112	400		
					56120	400		
PG1424+535	Z2T20204T	1166–1452	0.60	24			P1320401	243
HS1517+7403	Z2T20704T	1165–1451	0.60	24				
PG2131+066	Z2T20804T	1165–1451	0.60	18				
MCT0130-1937	Z2T20504T	1165–1451	0.60	17				
PG1707+427	Z2T20304T	1165–1451	0.60	20				
PG0122+200	Z2T20404T	1164–1450	0.60	18				
HS0704+6153	Z2T20604T	1165–1461	0.60	27				
	Z2T20605T	1165–1461	0.60	27				
KPD 0005+5106	Z27J0106T	1227–1263	0.06	13	26191	420	M1070201	132
	Z27J0107T	1273–1309	0.06	11	52108	360	M1070202	77
	Z27J0108T	1343–1379	0.06	16	52146	425	M1070203	138
					52185	425	P1040101	114
PG1034+001	Z0YE0C08T	1185–1221	0.06	5	18509	330		
	Z0YE0C09T	1221–1256	0.06	10	26201	262		
	Z0YE0C0AT	1369–1406	0.06	5				
	Z0YE0C0CT	1532–1568	0.06	5				
	Z0YE0C0DT	1622–1658	0.06	5				
HZ21	Z3GM0404T	1227–1265	0.06	42	31287	1147		
	Z3GM0405T	1339–1375	0.06	33				
HD149499B	Z3GM0504P	1227–1265	0.06	7	06272	90		
	Z3GM0505P	1338–1375	0.06	7	13781	40		
	Z3GM0506P	1699–1735	0.06	9	13782	28		
					13783	89		
					17467	75		

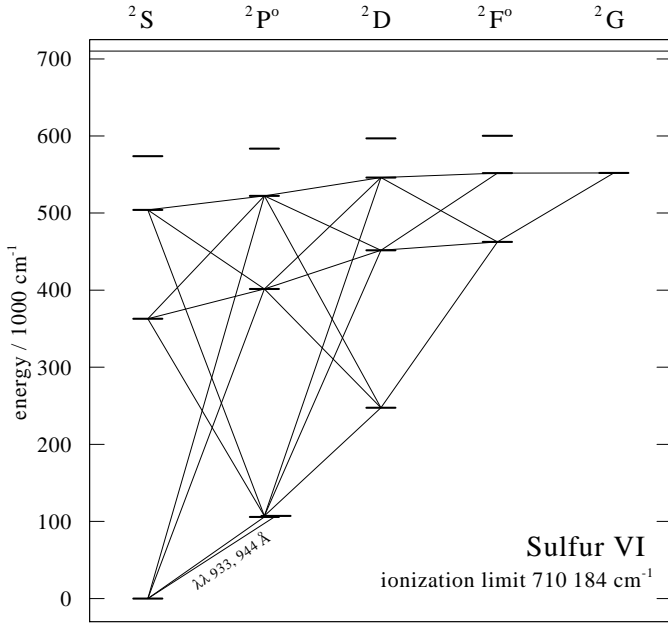


**Fig. 1.** Model atom for S VI. The transition responsible for the S VI resonance doublet in the FUSE range is labeled

spacecraft across the spectrograph apertures during each exposure. The resulting resolution was about  $24 \text{ km s}^{-1}$ .

## 2.2. HST and IUE

HST data was retrieved from the MAST. The spectra were taken with the Goddard High Resolution Spectrograph (GHRS) with a resolution of  $0.06 \text{ \AA}$  or  $0.6 \text{ \AA}$ . All exposures were made in the FPSPLIT mode which results in four individual spectra. As only the first exposure was wavelength-calibrated, the subsequent exposures were adjusted in wavelength to match the first using cross-correlation.

Reduced SWP spectra were extracted from the IUE Final Archive using preview data. They cover a wavelength range of  $1150\text{--}1980 \text{ \AA}$ , with a resolution of about  $0.1 \text{ \AA}$ . If more than one spectrum was available they were co-added using the S/N-ratio as weighting factor.

## 3. Model atmospheres and synthetic spectra

We have calculated a plane-parallel model atmosphere in radiative and hydrostatic equilibrium for each program star with our ALI code (Werner & Dreizler 1999) which can handle line blanketing by the iron group elements. We use the line list of Kurucz (1991). In general the models are similar to those of Deetjen et al. (1999), so we will restrict ourselves to a summary of the model atoms in Table 3. However, higher ionization stages of iron are taken into account due to the higher effective temperature of our program stars.

Sulfur line formation calculations were performed for the central star of K 1-16. The sulfur model atom

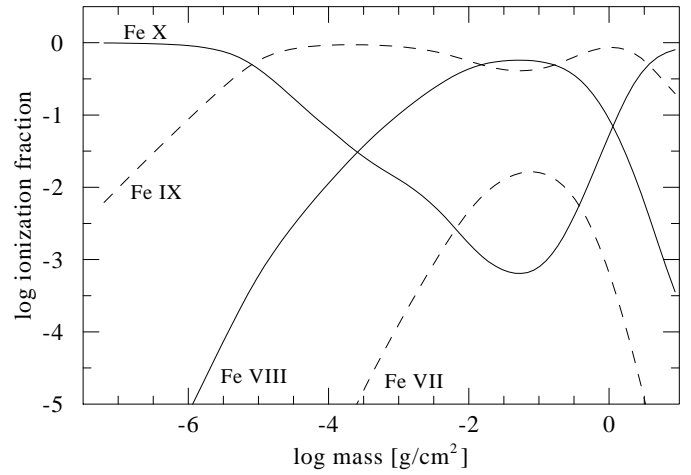


**Fig. 2.** Ionization structure of the model atmosphere for K 1-16 with  $T_{\text{eff}} = 140\,000 \text{ K}$ ,  $\log g = 6.4$  and a solar iron abundance

(S IV–VII) has been constructed using the Opacity Project (OP, Seaton et al. 1994) database which is a basic source for energy levels, oscillator strengths, and photoionization cross-sections. Since the OP energy levels are slightly different from laboratory measurements, we have replaced these values by those listed in Bashkin & Stoner (1975). The Grotrian diagram in Fig. 1 shows the levels and line transitions of the S VI model ion.

## 4. Iron abundance

For most of the objects the quality of the spectroscopic data is not sufficient to detect iron lines when compared with models with solar Fe abundance (all abundance values are given in mass fractions unless otherwise noted). For these objects we can only conclude that the iron abundance is less or equal solar (Table 1).

### 4.1. PG1159 stars

Before we discuss individual objects, we briefly go into those stars for which a solar abundance of Fe cannot be strictly excluded.

For PG1707+427 the FUSE data is superior to the HST data, however, the S/N of the FUSE spectrum is still too poor to detect potential Fe VI and Fe VII lines. For PG1424+535, HS1517+7403, PG2131+066, MCT0130-1937, PG0122+200, and HS0704+6153 only HST data exist, but their resolution ( $0.6 \text{ \AA}$ ) is too low. For Abell 43 IUE and HST spectra exist, but with insufficient S/N and resolution, respectively. Hence, for all the objects mentioned in this paragraph, Fe lines remain hidden in the spectra if the abundance is solar.

In contrast to our model predictions no Fe VI or Fe VI/VII lines can be detected in the FUSE spectra of HS2324+397 and PG1520+525, respectively. We derive a slight underabundance of 0.5 dex, but due to the relatively low S/N we must accept that a solar Fe abundance can-

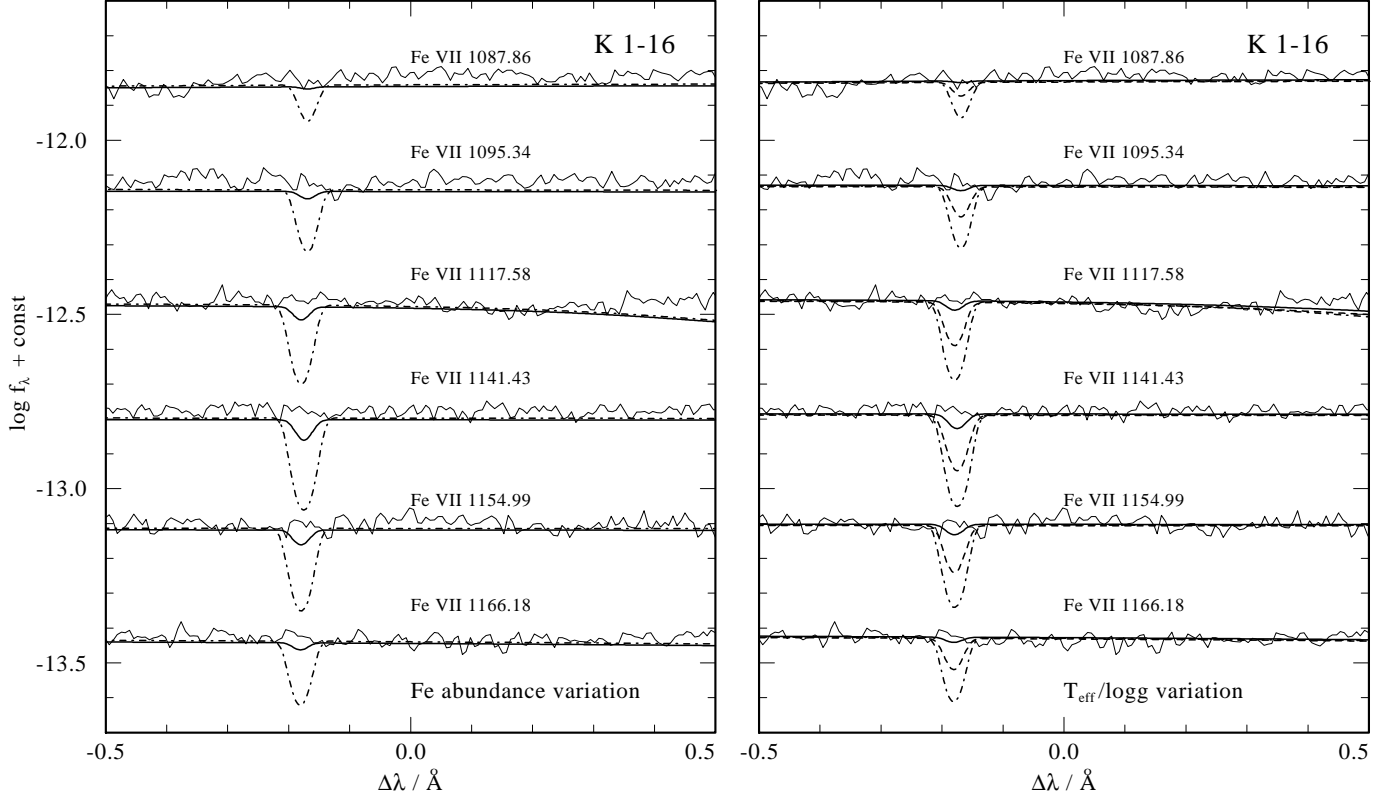


**Fig. 3.** The strongest iron lines expected in the FUSE data of K 1-16 are from Fe VII. None of these can be identified in K 1-16 (LiF2A data). Left panel: Models with  $T_{\text{eff}}=140\,000\text{ K}$ ,  $\log g=6.4$  and iron abundances of 0.1 solar (solid) and solar (dash-dotted line). Right panel: Models with  $T_{\text{eff}}=140\,000\text{ K}/\log g=6.4$  (dash-dotted),  $150\,000/6.5$  (dashed) and  $160\,000/6.6$  (solid), and solar iron abundance. A velocity shift of  $-48.07\text{ km s}^{-1}$  is taken into account according to Holberg et al. (1998). The spectra are smoothed with  $0.01\text{ Å}$  Gaussians

not be excluded rigorously. The HST data are not useful because of insufficient resolution ( $0.6\text{ Å}$ ).

For PG1159-035 four co-added IUE spectra were analyzed, with no clear detection of potential Fe VII lines. Also, Fe VII lines are not detectable in the FUSE spectra, hence, Fe is possibly underabundant by 0.5 dex or more.

#### 4.1.1. K 1-16

K 1-16 is an extremely hot PG1159 type central star. Due to its high effective temperature ( $140\,000\text{ K}$ ) the principal ionization stages of iron in the line formation regions of the atmosphere are Fe VIII and Fe IX (Fig. 2). A comparison of the excellent FUSE data with model spectra reveals, that Fe VII lines should be easily detectable if the effective temperature is indeed  $140\,000\text{ K}$  (Rauch & Werner 1997) and if the Fe abundance is solar. Fig. 3, however, shows that the strongest Fe VII model lines cannot be detected in the FUSE spectrum. Varying  $T_{\text{eff}}$  and Fe abundance in the model suggests that either the Fe abundance is lower than one tenth solar or that the effective temperature is higher than  $160\,000\text{ K}$ . The high  $T_{\text{eff}}$  would be surprising, because it means that the quoted value, which was determined from optical spectra, would be in error by at least  $20\,000\text{ K}$ . This is larger than a typical error of 10% for

such analyses, however, the high  $T_{\text{eff}}$  cannot be excluded definitely. Hence we conclude that an Fe underabundance of at least one dex is probably causing the failure to detect Fe VII lines in the FUSE data. Another argument for the Fe underabundance can be given. Two Fe IX lines with relatively large gf-values are known, which are located in the FUSE spectral region, contrary to most other lines of this ion, which are found in the  $100\text{--}600\text{ Å}$  region. These lines (at  $955.84\text{ Å}$  and  $973.71\text{ Å}$ ) clearly show up in the models with solar Fe abundance, but nothing is seen in the FUSE spectrum at these wavelengths (Fig. 4). This holds particularly for the hotter model ( $160\,000\text{ K}$ ), corroborating an underabundance even in the case that  $T_{\text{eff}}$  is higher than previously found.

A final decision about the possibility of an Fe underabundance in K 1-16 would require a high-precision analysis of He, C, O line profiles to fix  $T_{\text{eff}}$  as accurately as possible, using improved optical and UV spectroscopy in combination with the FUSE data. Alternatively, the search for the bulk of strongest Fe VIII and Fe IX lines in the  $100\text{--}200\text{ Å}$  range could be feasible with the Chandra observatory because K 1-16 is a soft X-ray source detected by ROSAT and EUVE.

The lack of Fe VII lines in the K 1-16 FUSE data supports a result by Holberg et al. (1998). They found no ev-

**Table 3.** Summary of the model atoms used in the model atmosphere calculations. The numbers in brackets give the individual line numbers summed into superlines for the iron ions. Each model atom is closed by a single NLTE level representing the highest ionization stage. These levels are not specified here

element	ion	NLTE levels	lines
H	I	5	6
He	I	1	0
	II	32	79
O	IV	1	0
	V	6	0
	VI	36	102
	VII	1	0
N	IV	6	4
	V	4	1
	VI	1	0
C	III	1	0
	IV	36	96
	V	1	0
Fe	III	7	25 (301 981)
	IV	7	25 (1 027 793)
	V	7	25 (793 718)
	VI	8	33 (340 132)
	VII	9	39 (86 504)
	VIII	7	27 (8 724)
	IX	8	32 (36 843)
total		184	494 (2 595 695)

idence of Fe VII lines in (much less meaningful) IUE spectra, contrary to earlier work by Feibelman & Bruhweiler (1990).

#### 4.1.2. RX J2117.1+3412

RX J2117.1+3412 is the hottest known PG1159-type central star ( $T_{\text{eff}}=170\,000\text{ K}$ ). From the discussion above it is clear, that the iron ionization is so high that Fe VII lines are not detectable, even in excellent data. This is indeed true when inspecting the FUSE spectra. It is interesting to note that earlier identifications of the Fe VII 1239.69 Å line in a high resolution HST/GHRS spectrum (Werner et al. 1996) and in IUE spectra (Feibelman 1999) are therefore most likely wrong. Our model predicts that none of the potential Fe VII lines in the GHRS and IUE range appears. We believe that the observed absorption is in fact an interstellar feature. There are two Mg II lines nearby, at 1239.93 Å and 1240.39 Å. The redshift of the photospheric spectrum (+47.22 km s<sup>-1</sup> from Holberg et al. 1998, confirmed by our measurement of the C IV 1107.93 Å line) and the blueshift of the ISM lines (-2.39 km s<sup>-1</sup>) conspire in a way that the interstellar Mg II 1239.93 Å line almost coincides with the position of a possible stellar Fe VII line. The same problem arises in the case of KPD 0005+5106 (see below). Generally, care must therefore be taken when iron

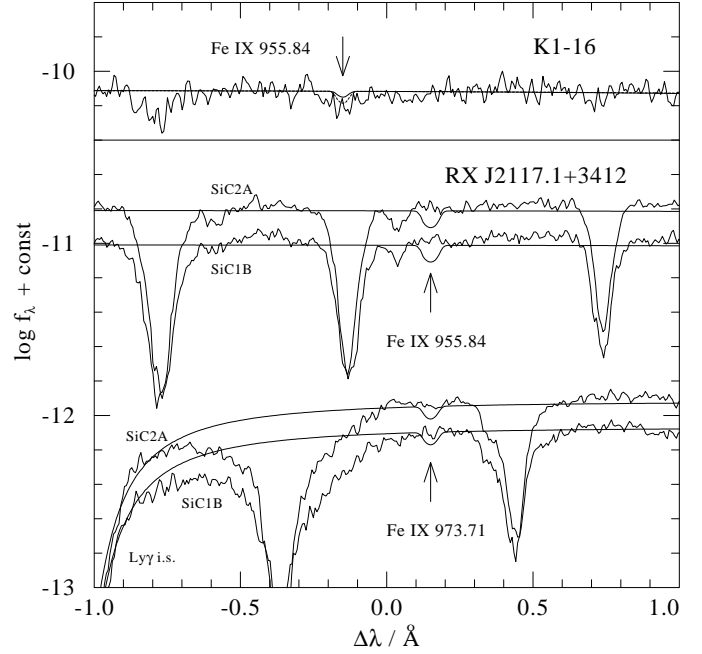


**Fig. 4.** Two Fe IX lines are located in the FUSE range. Top panel: K1-16 compared to two model spectra ( $T_{\text{eff}}=140\,000\text{ K}$ ,  $\log g=6.4$ , full;  $T_{\text{eff}}=160\,000\text{ K}$ ,  $\log g=6.6$ , dashed; solar Fe abundance) centered near the Fe IX 956 Å line. Bottom panel: RX J2117.1+3412 compared to the model with parameters as in Table 1 ( $T_{\text{eff}}=170\,000\text{ K}$ ,  $\log g=6.0$ , solar Fe abundance) centered around Fe IX 956 Å and Fe IX 974 Å. For this star both detector segments (SiC2A and SiC1B, slightly shifted vertically) are shown. The spectra are smoothed with 0.01 Å Gaussians. A radial velocity shift of +47.22 km s<sup>-1</sup> is taken into account

is identified in hot stars by means of this Fe VII 1239.69 Å line alone. This can only be regarded as safe when confusion with interstellar Mg II can be excluded. The two Fe IX lines introduced above cannot be identified in the FUSE spectrum (Fig. 4). Like in the case of K1-16 this could hint at an Fe underabundance and soft X-ray spectroscopy is required for a quantitative analysis.

#### 4.1.3. NGC 246

NGC 246 is also a very hot ( $T_{\text{eff}}=150\,000\text{ K}$ ) PG1159 type central star. Numerous IUE high resolution spectra exist which can be co-added. Holberg et al. (1998) find no evidence of the Fe VII lines reported by Feibelman & Bruhweiler (1990). We confirm this result and find that this is due to the high temperature. Better spectra (from HST or FUSE) might be able to detect these lines, which are weak but not completely absent in the solar Fe abundance models. It appears that the tentative identification of lines from even lower ionized Fe VI by Feibelman & Johansson (1995) and Feibelman (1995) is very likely not correct.

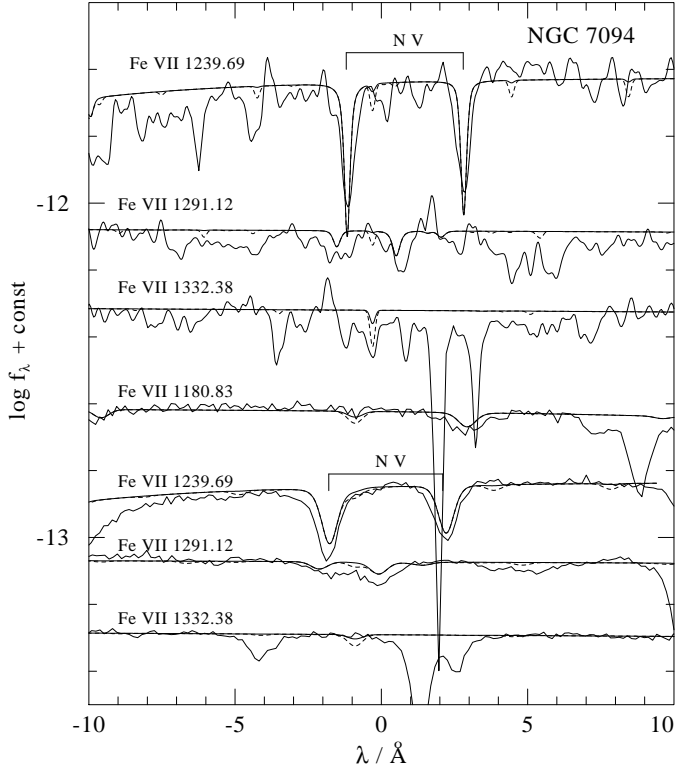


**Fig. 5.** The strongest Fe VII lines in the spectra of NGC 7094. The top three lines are fitted to IUE spectra, the four lines at the bottom are fitted to HST spectra. The models have iron abundances of 0.1 solar (solid line) and solar (dashed line). No iron lines can be identified. The IUE and HST spectra are smoothed 0.2 Å and 0.6 Å FWHM Gaussians, respectively. The calculated spectra were shifted accounting for radial velocity. Note that the radial velocity of the photospheric lines from HST data differs from that of the IUE data

#### 4.1.4. NGC 7094

NGC 7094 is a so-called hybrid PG 1159 star, meaning that detectable amounts of hydrogen are present in its atmosphere. We fail to detect iron lines in the IUE and HST spectra of NGC 7094 (Fig. 5). This is in contrast to Feibelman (2000), who claimed identification of several Fe VI and Fe VII lines in the IUE data. This central star is so hot that our model predicts stronger Fe VII than Fe VI lines. One can derive an underabundance of 0.5 dex. Inspecting the superior FUSE data we, again, cannot identify Fe VII lines. Comparison with our model reveals an even higher underabundance of 1–2 dex (Fig. 6).

#### 4.1.5. Abell 78

The central star of the planetary nebula Abell 78 is one of the rare [WC]–PG1159 transition object showing spectral signatures of both early [WC] spectral type (emission lines) and PG1159 type (absorption lines). As in the case of NGC 7094 only the FUSE spectrum allows one to determine a strict limit to the Fe abundance. A first analysis

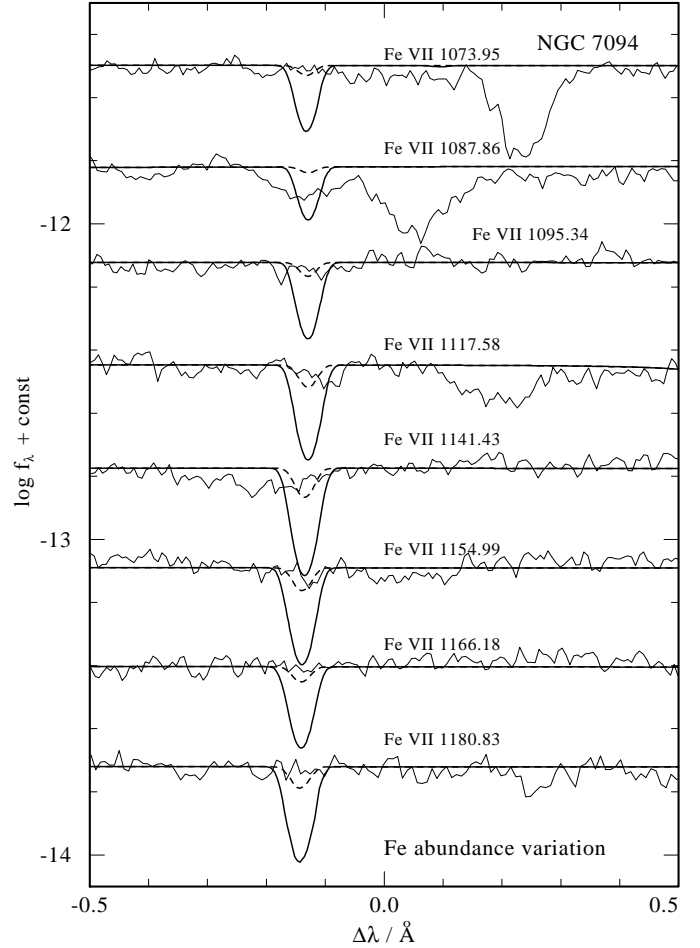


**Fig. 6.** Details of FUSE spectrum of NGC 7094 compared to theoretical line profiles, centered around the strongest Fe VII lines in the model. The model iron abundances are 0.1 solar and 0.01 solar. No iron lines are detectable in the FUSE spectrum. Spectra are smoothed with 0.01 Å Gaussians

has been presented recently by Werner et al. (2002) and the result is an underabundance of 1–2 dex.

## 4.2. DO white dwarfs

KPD0005+5106 is the hottest known DO white dwarf, showing peculiar emission lines due to ultrahigh ionized light metals (Werner & Heber 1992) and it is the only white dwarf known to have an X-ray corona (Fleming et al. 1993). An upper limit for the Fe abundance can be inferred from the GHRS spectrum (one tenth solar, Fig. 7). As in the case of RX J 2117.1+3412, the absorption feature near 1240 Å cannot stem from Fe VII, because no other Fe VII lines, neither in the HST nor in the FUSE data, are detectable. We derive an upper limit of  $\log(\text{Fe}/\text{He}) < -5$  (by number).

PG1034+001 is another hot DO white dwarf for which an iron abundance of  $\log(\text{Fe}/\text{He}) = -5$  has been derived from Fe VI lines in HST data (Werner et al. 1995). We confirm this result by our re-analysis.

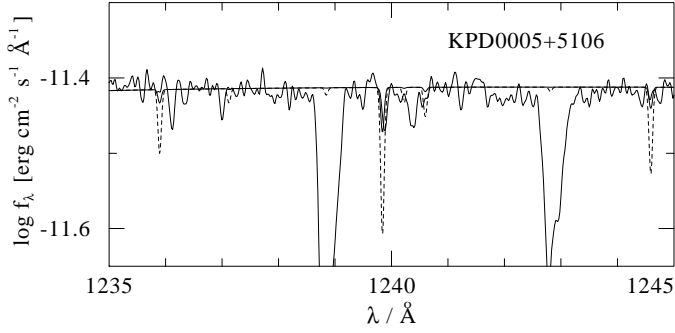


**Fig. 7.** The strongest Fe VII lines expected in the HST spectrum of KPD 0005+5106. We show models with an iron abundance of 0.1 solar (solid line) and solar (dashed line). No Fe lines can be identified. The feature at 1240 Å is probably interstellar Mg II. The HST spectrum is smoothed with 0.06 Å Gaussian. A radial velocity shift of +36.15 km s<sup>-1</sup> is taken into account (Holberg et al. 1998)

HZ 21 is one of the coolest DO white dwarfs. We confirm the result by Holberg et al. (1998) that only a single photospheric line can be identified in the IUE spectra (He II 1640 Å). The HST spectra are superior in quality, but they only cover wavelength ranges where Fe VI and Fe VII are located. HZ 21 is too cool to ionize iron this strongly. We derive an upper limit of  $\log(\text{Fe}/\text{He}) < -4$ .

HD149499B is also a cool DO star. From the absence of Fe V lines in the HST spectrum we derive an upper limit for the Fe abundance:  $\log(\text{Fe}/\text{He}) < -5$ .

To conclude our results on the DO stars, the iron abundance is much lower than predicted by diffusion theory (Fig. 8), confirming earlier results on other DO white dwarfs (Dreizler 1999).

#### 4.3. Summary of iron line analyses

To summarize this section, we fail to identify iron lines in any PG1159 star. In most objects this is compatible with a solar iron abundance. In three cases (PG1159-035, HS2324+397, PG1520+525) we tentatively propose an interpretation in terms of a slight iron underabundance (0.5 dex). In three cases (K 1-16, NGC 7094, Abell 78) the underabundance is estimated to 1–2 dex.

For three out of four DO white dwarfs investigated in this work we derive an upper iron abundance limit from the absence of respective lines in their spectra. In the case of PG1034+001 the analysis of detected iron lines corroborates an earlier abundance determination.

### 5. Detection of sulfur in K 1-16 and other PG 1159 stars

The FUSE spectrum of K 1-16 allows for the first identification of sulfur in a PG1159 star based on the 933.38/944.52 Å resonance doublet (Fig. 9). It seems that both lines are split into two components, especially the S VI 933.38 Å line. The stronger blueshifted components

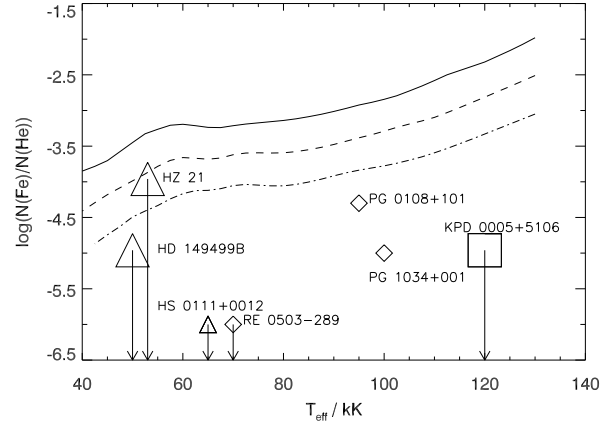


**Fig. 8.** Comparison of predicted iron abundances to our results for the DO white dwarfs. The graphs show diffusion equilibrium abundances for iron at  $\tau = 2/3$  as calculated by Chayer et al. (1995):  $\log g = 7.0$  (solid line),  $\log g = 7.5$  (dashed),  $\log g = 8.0$  (dash-dotted). The symbols mark objects with  $\log g = 7.0$  ( $\square$ ),  $\log g = 7.5$  ( $\diamond$ ) and  $\log g = 8.0$  ( $\triangle$ ). Small symbols mark the objects analyzed by Dreizler (1999)

are attributed to the photosphere. Their velocity shift is about  $-40 \text{ km s}^{-1}$  which is in coarse agreement with measurements from IUE spectra ( $-48.07 \text{ km s}^{-1}$ , Holberg et al. 1998). Our model fit suggests a solar sulfur abundance.

The S VI doublet is also detected in the spectra of RX J 2117.1+3412, PG1520+525, and PG1159-035.

### 6. Discussion

Whether the iron deficiency in PG1159 stars is related to the same phenomenon observed in metal-poor post-AGB B-A-F supergiants can only be speculated upon. In some cases dust fractionation on the AGB has been invoked to explain the Fe deficiency (Van Winckel et al. 1992), whereas in other cases evidence was found that iron was transformed to heavier elements by s-process neutron captures (Decin et al. 1998). To our opinion it is unlikely that dust fractionation on the AGB is responsible for the iron deficiency in PG1159 stars, because strong post-AGB mass-loss removes layers “cleaned” from iron during the AGB phase.

In the case of PG1159 stars the high C and O abundances result from envelope mixing caused by a late He-shell flash (Herwig et al. 1999). This event also modifies the near-solar abundance ratios of iron-peak elements in the envelope by dredging up matter in which s-process elements were built-up by n-capture on  $^{56}\text{Fe}$  seeds during the AGB phase. This scenario can be tested by analyzing the resulting Fe/Ni abundance ratio, because it is significantly changed in the intershell region in favor of Ni by the conversion of  $^{56}\text{Fe}$  into  $^{60}\text{Ni}$ . The Fe depletion by n-captures typically amounts to a factor of 10 (Busso et al. 1999).



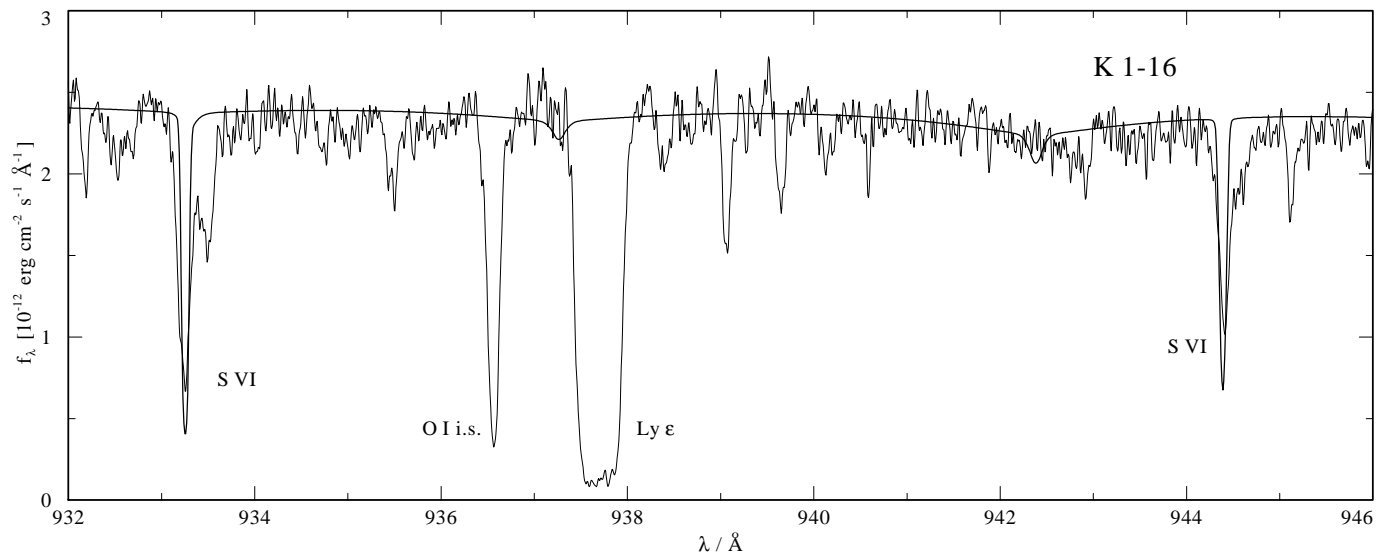


**Fig. 9.** Line profile fit to the S VI resonance doublet in the FUSE spectrum of K 1-16. The model has a solar sulfur abundance. Other parameters as in Table 1. The spectra are smoothed with  $0.02 \text{ \AA}$  Gaussians

In order to roughly estimate the Ni/Fe ratio one can assume nuclear statistical equilibrium. The two most abundant Ni isotopes are  $^{60}\text{Ni}$  (26%) and  $^{58}\text{Ni}$  (68%). During s-process  $^{58}\text{Ni}$  is destroyed (and not synthesized), by conversion into  $^{60}\text{Ni}$ .  $^{60}\text{Ni}$  is converted to heavier elements 4 times faster than it is produced from  $^{56}\text{Fe}$ . Consequently, a ratio  $\text{Fe}/\text{Ni} \approx 4$  results, which is a factor of five below the solar value. This could be detected by high resolution HST and FUSE UV spectroscopy of PG1159 stars, but only in objects that are cooler than the three hot stars for which the strong Fe deficiency has been found. This is because in the hot PG1159 stars Ni VII lines are the prevailing nickel features but they are located in the inaccessible EUV region. Interestingly, Asplund et al. (1999) have indeed found that in Sakurai's object, which is thought to undergo a late He-shell flash, Fe is reduced to 0.1 solar and  $\text{Fe}/\text{Ni} \approx 3$ . This and other s-process signatures might also be exhibited by Wolf-Rayet central stars and PG1159 stars.

More quantitative results from nucleosynthesis calculations in appropriate stellar models have been presented recently (Herwig et al. 2002) and inclusion of nuclear networks in evolutionary model sequences will become available in the near future.

Most recent results presented at the IAU Symposium 209 (Planetary Nebulae, Canberra) confirm that iron deficiency among H-deficient post-AGB stars is not restricted to PG1159 stars, as can be expected from evolutionary considerations. As already mentioned, the [WC]-PG1159 transition object Abell 78 is iron deficient (Werner et al. 2002) and three Wolf-Rayet central stars are iron deficient, too. Gräfener et al. (2002) report a low Fe abundance in SMP 61, an early type [WC5] central star in the LMC. Its abundance is at least 0.7 dex below the LMC metallicity. Crowther et al. (2002) find evidence for an iron un-

derabundance of 0.3–0.7 dex in the Galactic [WC] stars NGC 40 ([WC8]) and BD+30 3639 ([WC9]).

A general iron deficiency among PG1159 stars would also have implications for asteroseismology. Roughly half of all PG1159 stars are GW Vir pulsators and frequency analyses have revealed interesting results about the interior structure of these stars (e.g. Winget et al. 1991). There is still a debate about details of the pulsation driving mechanism. While it is accepted that cyclic ionization of carbon and oxygen just beneath the photosphere is the main driver, the iron opacity also does play a role (Saio 1996). In light of our iron abundance analysis of the pulsator K 1-16 it would be interesting to re-address the problem of pulsation driving.

*Acknowledgements.* We thank Falk Herwig for useful discussions. HST data analysis in Tübingen is supported by the DLR under grant 50 OR 9705 5. JLD is supported by the DFG under grant We 1312/23-1.

## References

- Asplund M., Lambert D.L., Kipper T., Pollacco D., & Shetrone M.D. 1999, *A&A*, 343, 507
- Bashkin S., & Stoner J.O. Jr. 1975, *Atomic Energy Levels And Grotrian Diagrams*, North-Holland/American Elsevier
- Busso M., Gallino R., & Wasserburg G.J. 1999, *ARA&A*, 37, 239
- Chayer P., Fontaine G., & Wesemael F. 1995, *ApJS*, 99, 189
- Crowther P.A., Abbott J.B., Hillier D.J., & De Marco O. 2002, in *Planetary Nebulae*, ed. M. Dopita et al., IAU Symp. 209, ASP Conference Series, in press
- Decin L., Van Winckel H., Waelkens C., & Bakker E.J. 1998, *A&A*, 332, 982
- Deetjen J.L., Dreizler S., Rauch T., & Werner K. 1999, *A&A*, 348, 940
- Dreizler S. 1999, *A&A*, 352, 632
- Dreizler S., & Werner K. 1996, *A&A*, 314, 217
- Dreizler S., & Heber U. 1998, *A&A*, 334, 618

- Dreizler S., Werner K., Heber U., & Engels D. 1996, *A&A*, 309, 820
- Dreizler S., Werner K., & Heber U. 1997, in *Planetary Nebulae*, ed. H.J. Habing and H.J.G.L.M. Lamers, IAU Symp. 180, Kluwer, p.103
- Feibelman W.A. 1995, *PASP*, 107, 531
- Feibelman W.A. 1999, *ApJ*, 513, 947
- Feibelman W.A. 2000, *ApJ*, 542, 957
- Feibelman W.A., & Bruhweiler F.C. 1990, *ApJ*, 357, 548
- Feibelman W.A., & Johansson S. 1995, *ApJS*, 100, 405
- Fleming T.A., Werner K., & Barstow M.A. 1993 *ApJL*, 416, 79
- Gräfener G., Hamann W.-R., & Peña M. 2002, in *Planetary Nebulae*, ed. M. Dopita et al., IAU Symp. 209, ASP Conference Series, in press
- Herwig F., Blocker T., Langer N., & Driebe T. 1999, *A&A* 349, L5
- Herwig F., Lugaro M., & Werner K. 2002, in *Planetary Nebulae*, ed. M. Dopita et al., IAU Symp. 209, ASP Conference Series, in press
- Holberg J.B., Barstow M.A., & Sion E.M. 1998, *ApJS*, 119, 207
- Kruk J.W., & Werner K. 1998, *ApJ*, 502, 858
- Kurucz R.L. 1991, in *Stellar Atmospheres: Beyond Classical Models*, ed. L. Crivellari, I. Hubeny, D.G. Hummer, NATO ASI Series C, Vol. 341, p.441
- Moos H.W., Cash W.C., Cowie L.L. et al. 2000, *ApJL* 538, 1
- Napiwotzki R., Hurwitz M., Jordan S., et al. 1995, *A&A*, 300, L5
- Rauch T., & Werner K. 1997, in *The Third Conference on Faint Blue Stars*, ed. A.G.D. Philip, J. Liebert, R.A. Saffer, (L. Davis Press, Schenectady, NY), p.217
- Sahnou D.J., Moos H.W., & Ake T.B. 2000, *ApJL* 538, 7
- Saio H. 1996, in *Hydrogen-Deficient Stars*, ed. U. Heber, C.S. Jeffery, ASP Conference Series 96, 361
- Seaton M.J., Yu Yan, Mihalas D., & Pradhan A.K. 1994, *MNRAS*, 266, 805
- Van Winckel H., Mathis J.S., & Waelkens C. 1992, *Nature*, 356, 500
- Werner K. 1996, *A&A*, 309, 861
- Werner K. 2001, in *Low mass Wolf-Rayet stars: Origin and evolution*, ed. T. Blocker, L.B.F.M. Waters, A.A. Zijlstra, *Ap&SS*, 275, 27
- Werner K., & Heber U. 1992, in *Atmospheres of Early-Type Stars*, ed. U. Heber, C.S. Jeffery, *Lecture Notes in Physics* 401 (Springer, Berlin), p.291
- Werner K., & Koesterke L. 1992, in *Atmospheres of Early-Type Stars*, ed. U. Heber, C.S. Jeffery, *Lecture Notes in Physics* 401, (Springer, Berlin), p.288
- Werner K., & Dreizler S. 1999, in *Computational Astrophysics*, ed. H. Riffert, K. Werner, *J. Comp. Appl. Math.*, 109, 65
- Werner K., Heber U., & Hunger K. 1991, *A&A*, 244, 437
- Werner K., Dreizler S., & Wolff B. 1995 *A&A*, 298, 567
- Werner K., Dreizler S., Heber U., et al. 1996, *A&A*, 307, 860
- Werner K., Dreizler S., Koesterke L., & Kruk J.W. 2002, in *Planetary Nebulae*, ed. M. Dopita et al., IAU Symp. 209, ASP Conference Series, in press
- Winget D.E., Nather R.E., Clemens J.C., et al. 1991, *ApJ*, 378, 326